Case Studies in Construction Materials 22 (2025) e04136

Contents lists available at ScienceDirect

Case Studies in Construction Materials

journal homepage: www.elsevier.com/locate/cscm

Machine learning-based prediction of torsional behavior for ultra-high-performance concrete beams with variable cross-sectional shapes

Elhabyb Khaoula [a], Baina Amine [a], Bellafkih Mostafa [a], A. Deifalla [b,*], Amr El-Said [c], Mohamed Salama [d], Ahmed Awad [e]

[a] RAISS Lab, National Institute of Posts and Telecommunications - INPT Rabat, Morocco
[b] Structural Engineering and Construction Management Department, Future University in Engineering, Cairo 11835, Egypt
[c] Department of Civil Engineering, The Higher Institute of Engineering, El Shrouk, Cairo, Egypt
[d] Department of Civil Engineering, Modern Academy for Engineering and Technology, Cairo, Egypt
[e] Faculty of Engineering, October University for Modern Sciences and Arts, Giza, Egypt

ARTICLE INFO

Keywords:
Ultra-high-performance concrete
Torsion strength
Machine learning
Supervised learning
Smart constructures

ABSTRACT

Ultra-high-performance concrete (UHPC) is renowned for its exceptional mechanical properties; however, its torsional behavior remains inadequately understood, posing challenges for its application in structures subjected to twisting loads. Existing prediction methods often fall short of accurately capturing the complex interplay between material characteristics, cross-sectional geometry, and reinforcement, leading to significant errors. This work introduces a unique Machine Learning (ML) method to accurately anticipate the torsional behavior of UHPCs. Three powerful algorithms, Random Forest, Gradient Boosting Regressor, and Long Short-Term Memory (LSTM), were trained and assessed on a dataset of 113 UHPC specimens. The best R-squared was 99 % provided by the Gradient Boosting Regressor, while the LSTM and Random Forest showed 98 % and 96 % accuracy. The ML approach determined that splitting tensile strength, fiber length, web width, and stirrup diameter were the most important factors controlling torsional force. These results provide insight into the complex interaction affecting UHPC torsional performance, opening the path for accurate UHPC design in challenging applications.

1. Introduction

The recent emergence and quick advancement of the use of Ultra-high-performance Concrete can be highly attributable to the numerous and superior properties it

has compared to conventional concrete. UHPC has better compressive strength of up to 120 MPa, great toughness, and excellent durability use and combines several properties to rank it as an utter superior material for a wide range of applications [1–5]. UHPC's durability, combined with its excellent strength-to- weight ratio, enables it to form longer spans and thinner sections, yielding leaner

* Corresponding author.
E-mail addresses: elhabyb.khaoula@doctorant.inpt.ac.ma (E. Khaoula), baina@inpt.ac.ma (B. Amine), bellafkih@inpt.ac.ma (B. Mostafa), ahmed.deifalla@fue.edu.eg (A. Deifalla), a.elsayed@sha.edu.eg (A. El-Said), m.salama@eng.modern-academy.edu.eg (M. Salama), amosad@msa.edu.eg (A. Awad).

https://doi.org/10.1016/j.cscm.2024.e04136
Received 24 July 2024; Received in revised form 7 December 2024; Accepted 16 December 2024
Available online 24 December 2024

and more aesthetically pleasing buildings [6,7]. As a high performance material, it is, in particular, ideal for structures such as high rises, bridges, and offshore platforms among others [8]. Despite the growing interest in UHPC however, the investigations have concentrated mostly on other parameters, namely, its compressive strength, tensile strength and elastic modulus among others [9–17]. These studies are important in explaining the mechanical properties of the material, but the research dealing with its flexural and shear behaviors has been limited [18–23]. The studies on torsional behavior for UHPC structures are not numerous, but it is imperative to study these twisting loads such as those associated with wind and seismic loading [24–34]. This limited knowledge constitutes a major barrier to the successful exploitation of UHPC and its use in various structural elements. Quite recently, some research attempts have provided new information that enlarges the existing knowledge of UHPC torsional behavior and pivots essential further developments concerning the design and application of UHPC in structural elements. In most of the studies steel fibers were consistently shown to improve torsional performance of UHPC composites. Zhou et al. [24], Al.Khuzaie et al. [25], and Yang et al. [26] all observed that the cracking torque and ultimate torque increased significantly with an increase in steel fiber volume percentage. This phenomenon was due to steel fibers' very high tensile strength and ability to tie cracks, thus inhibiting the formation or growth of cracks. Remarkably, Zhou et al. [24] found that the use of 2 % steel fibers led to an increase of 79 % in cracking torque and 159 % in ultimate torque; Al. Khuzaie et al. [25] on the other hand found that with only 2 % steel fibers added to a hollow T-beam, cracking torque increased by 184 % while the ultimate torque increased by 66 %. In another study conducted by Yang et al. [26], when the fiber content was increased from 1 % to 2 %, they reported a 19 % and a 27 % increase in cracking and ultimate torque, respectively. Specifically, Zhou et al. [27] observed that further increasing the fiber content to more than 1.5 % rendered positive but marginal effects, indicating that there is a general limit in the quantity of fibers that can be added effectively for the enhancement of torsional loading capacity.

The torsional response of UHPC is also affected by the cross-sectional shape and the existence of a flange. Cross-sectional size, wall thickness, and cross-sectional shape categories have all been observed to impact the hollow UHPC beams' torsional resistance and rigidity [25,27,28]. However, the cross-sectional dimensions are the most important for the cracking torque, while it is less affected by the wall thickness and the cross-sectional shape. The flange presence can increase the torsional strength and lower the torsional deformations Fig. 15 of UHPC hollow beams [27,29]. Al.Khuzaie et al. [25] revealed that in the presence of a mounted flange, the angle of inclination increased and the size of main cracks decreased suggesting

more ductile failure. Further, Zhou et al. [27] discovered that it can also enhance the overall torsional strength of the beam by preventing first diagonal cracking, which is catastrophic in nature.

Although steel fibers were the primary components that improved the torsional behavior of the composite materials, other factors contributed as well. Kwahk et al. [30] research demonstrating that in the case of torsional loads, steel fibers were superior to stirrups in resistance to torsional cracking and torsional strength, thus providing a basis for the reasoned need for increase in fiber density to improve structural stability without mounting stirrups. Nevertheless, in contrast, Cao et al. [31] noticed that on the contrary there were little to no effects of stirrups on cracking torque but rather maintained a proper crack width while boosting the plastic stiffness and concluded that the performance and ductility requirements on torsion steels may be met by using steel fibers with stirrups. In line with this, Yang et al. [26] noted that in the case of UHPC square beams having 1 % steel fibers, if the stirrup ratio is increased from 0 % to 0.70 %, the ultimate torque is improved by 18 %. This rise was even more significant, at 66 %, for beams having 2 % steel fibers. It was also seen that the effect of longitudinal reinforcement was rather less concerning cracking torque being very minimal and even decreasing the torsional ductility [31]. To date, very few phases of this problem have been adequately solved, and predicting the torsional behavior of UHPC seems to be even more complex due to the synergetic relations among the materials comprising the beam, beam geometry, and additional reinforcement. The available theoretical models will make good estimates of the cracking torque and stabilizing torque [27,28] but do not go far beyond those parameters thus giving unpardonably low values of ultimate torque prediction, these limitations highlight the urgent need for models that take into account the current complicated dynamics. The conventional analytical frameworks usually prove inadequate as they are not able to account for the non-linearity and many factors that affect the torsional behavior of UHPC. Furthermore, given that mix proportions and other manufacturing aspects can vary considerably, the development of predictive models that fit all situations is impossible. This justifies the shift in focus to more flexible data-driven methodologies. In this instance, machine learning (ML) can be a potential remedy to this problem. Given the comprehensive understanding of organizational premise, material composition and structure, shape and type of loading etc., gage where ML input uses databank oriented for learning of torsional properties and their dependence on the input factors. As a result, this allows for the creation of sturdy and predictive designs that encourage the healthy and accurate forecasting of torsional properties of UHPC [35–37]. In this article, we will begin with a detailed literature review that explores various machine learning techniques employed to identify the characteristics of different types of concrete, including Ultra-High-Performance Concrete (UHPC), High-Performance Concrete (HPC), and Reinforced Concrete (RC). Following this, the methodology section will describe the data collection process, which involved compiling our database from multiple studies in the UHPC field. After detailing the steps taken to clean and preprocess the database, we will outline the implementation of the selected

machine learning algorithms for predicting the torsional strength of UHPC structures. The results and discussion sections will present our findings regarding these predictions, highlighting the parameters identified and their respective influences on torsional strength. Finally, the conclusion will provide a comprehensive summary of our research outcomes and suggest avenues for future exploration.

2. Literature review

Machine learning focuses on creating analytical models that adapt and improve based on data, contrasting with traditional programming that uses explicit instructions. This technology has advanced applications in areas such as predicting material properties and

Table 1
Summary of Research Works on Different Concrete Types and Prediction Models.

Authors Suppressed Due to Excessive Length	**Research Works**	**Material Type**	**Predicted Property**	**Used Dataset**	**Algorithm**	**Performance Metrics**	**Best model**	**Future Work**
	[38]	UHPC	Flexural Strength	317 data points from UHPC database with 21 input factors	SVM, MLP, GBM	R^2, MSE, MAE	GBM	Further Exploration of Raw Ingredients, Validation in Real-World Scenarios
	[39]]	FAGC	Compressive Strength	114 sets Fly Ash-Based Geopolymer Concrete	DT, RF, Bagging	R^2, MAE	BM	Implementation of Artificial Neural Networks
	[40]	AAC	Strength and Fresh Properties	73samplesofalkali activated concrete mixtures	RF	$_R2$	RF	Incorporating Additional Variables
	[41]]	SCC	Compressive Strength	515 samples of SCC with recycled aggregates	LGBM, RF	RMSE, MAE, $_R2$	RF	Improving Model Performance, Implementing RF for Another Concrete Type
	[42]	UHPFRC	Compressive Strength	130 UHPFRC dosages with information on uniaxial tensile behavior	LSTM	MAPE, R^2	LSTM	Inclusion of Supplementary Materials, Comparison of Different Machine Learning Algorithms
	[43]	WAC	Stress Strain	1030 sets of compressive strength of concrete	LSTM, ANN	MSE, RMSE	LSTM	Not Listed
	[44]	UHPC	Flexural Strength	30 different concrete mixtures	Gradient Boost, XGB , AdaBoost	R^2, MSE	LSTM	Increasing Input Variables and Database
	[45]	GSCC	Mechanical Properties Modeling	105 data samples of GSCC	ANN, RNN	MSE, MAE, RMSE	RNN	Predicting Additional GSCC Qualities, Improving Performance
	[46]	AM	Dynamic Modules	16 asphalt concrete mixtures with binders and limestone aggregates	XGBoost, AdaBoost	MAPE, RMSE, MSE	XGB	Expanding Research Scope
	[26]	UHPC	Dynamic Compressive Strength	Not mentioned	RF, LGBM, RNN	MAPE, RMSE	LSTM	Expanding the Research Scope
	[47]	RC	Torsional Capacity	287 RC specimens with varyingcross-sectional shapes and dimensions	XGBM, SVR, RF, BPANN	R^2, MSE, RMSE	XGB	Expanding Dataset for Wider Variety of RC, Integrating Hybrid Machine Learning Techniques
	[48]	RC	Compressive Strength	159 RC specimens with solid and hollow sections	RF, DT, SVR	RMSE, MAPE, MAE	RF	Including Various Types of RC Structures and Environmental Conditions

optimizing structural performance. While it empowers researchers to process large datasets and identify patterns, human interpretation remains essential. In this study, we emphasize supervised learning, specifically regression, to predict the torsional strength of ultra-high-performance concrete (UHPC) based on various influencing factors. Our literature review will verify the application of machine learning techniques in the context of UHPC and other types of concrete, providing insights into how these methods enhance predictions of concrete performance. This review will be summarized in Table 1.

Recent studies underscore the increasing significance of machine learning (ML) techniques in predicting the mechanical behavior of advanced concrete materials. Qian et al. [38] employed ML algorithms, including Support Vector Machines (SVM), Multi-Layer Perceptrons (MLP), and Gradient Boosting Machines (GBM), to forecast the flexural strength of ultra-high-performance concrete (UHPC). Their findings indicated that the GBM model significantly outperformed SVM and MLP, achieving a Mean Absolute Error (MAE) of 1.9. In a related study, Ahmad Ayaz et al. [39] applied ML algorithms such as Decision Trees (DT), Adaptive Boosting (AR), and Bagging (BR) to predict the compressive strength of geopolymer concrete, reporting R^2 values exceeding 0.9, which highlights ML's capability to manage nonlinear relationships and variability in material composition. Sun et al. [40] demonstrated the effectiveness of the Random Forest algorithm in optimizing the strength and fresh properties of alkali-activated concrete (AAC). The models achieved R^2 values ranging from

0.92–0.96 for the training set and 0.89–0.94 for the test set, confirming a strong correlation between design parameters and performance metrics, such as compressive strength and slump values. Furthermore, De-Prado-Gil et al. [41] expanded ML applications to self-compacting concrete (SCC) using recycled aggregates, employing algorithms such as k nearest neighbor (KNN), Random Forest (RF) and Light Gradient Boosting Machine (LGBM). Their results revealed that LGBM outperformed the other models with a root mean square error (RMSE) of 6.01. The inclusion of recycled materials introduced variability in mechanical properties, complicating predictions for simpler models.

Jin et al. [42] developed a novel approach for optimizing concrete mix ratios using a combination of Long Short-Term Memory (LSTM) algorithms and Multi objective particle swarm optimization. Their study focused on balancing

strength, material costs, and carbon emissions, with the LSTM model demonstrating high accuracy in predicting compressive strength. Tanhadoust et al. [43] further showcased LSTM's capability by accurately predicting the stress-strain relationships of normal and lightweight aggregates at elevated temperatures, achieving an R^2 value of 0.96. Similarly, Wang et al. [44] applied Gradient Boosting, AdaBoost, and Extreme Gradient Boosting (EGB) to predict the flexural strength of ultra-high-performance concrete (UHPC), achieving R^2 values up to 0.95. They also employed SHAP analysis to assess the impact of input variables, enhancing the optimization of materials for targeted structural applications. In a related investigation, Ayvore et al. [45]integrated Genetic Programming (GEP) and Artificial Neural Networks (ANN) to effectively model the mechanical properties of self-compacting concrete, achieving a notable accuracy with an R^2 value of 1.09. This research exemplifies the capability of machine learning algorithms to handle nonlinear relationships among input parameters in the context of sustainable concrete development. Additionally, the combination of Random Forest (RF) and Support Vector Machines (SVM) in predicting the performance of recycled aggregate concrete produced robust outcomes, with R^2 values ranging from 0.85 to 0.95, thereby reinforcing the utility of these methodologies in material recycling applications. Ali et al. [46] further explored the potential of the XGBoost algorithm to estimate the dynamic modulus of asphalt mixtures for flexible pavements, yielding commendable predictive performance characterized by an average Mean Absolute Error (MAE) of 2243 MPa, a Root Mean Square Error (RMSE) of 3035 MPa, and an R^2 of 0.86.

In parallel, Khuzaie et al. [26] examined the influence of various factors, including steel fiber proportions, beam geometries, reinforcement ratios, and silica fume content, on the ultimate torsional capacity of reinforced concrete beams. By leveraging artificial intelligence, specifically ANN, they successfully modeled the stress-strain relationships derived from experimental data, establishing ANN as the most precise model for predicting torsion capacity, outpacing traditional regression methodologies. Furthermore, Hematibahar et al. [47] provided insights into the distinctions between high-performance concrete (HPC) and ultra-high-performance concrete (UHPC), while investigating optimal machine learning techniques to predict their mechanical properties. Utilizing a dataset of over 400 concrete mixes, their study employed various algorithms, including Partial Least Squares (PLS) regression, linear regression, and Lasso regression, revealing that PLS achieved a determination coefficient (R^2) exceeding 93 %, thereby validating its efficacy in predicting critical properties such as strength and durability.

Overall, these cumulative findings highlight the growing significance of machine learning methodologies in designing and optimizing advanced construction materials. The advanced models, particularly GBM, and LSTM demonstrate considerable effectiveness in predicting and optimizing the mechanical behavior of high-performance concretes, while adeptly addressing the complexities inherent in the interactions among input variables.

3. Methodology

This research focuses on predicting the torsional strength of Ultra-High-Performance Concrete (UHPC) using machine learning (ML) techniques. By implementing Random Forest, LSTM, and Gradient Boosting Regressor algorithms, the study introduces ML approaches in this field to achieve accurate predictions. A well-defined set of 30 UHPC attributes—such as geometric dimensions, reinforcement characteristics, and material properties—serve as predictors, helping clarify complex relationships and assess each parameter's influence on torque capacity. The research begins with thorough data preparation to address any data weaknesses, streamlining the training and testing stages. Each model's performance is then evaluated through validation metrics discussed in the following section.

1. Dataset collection

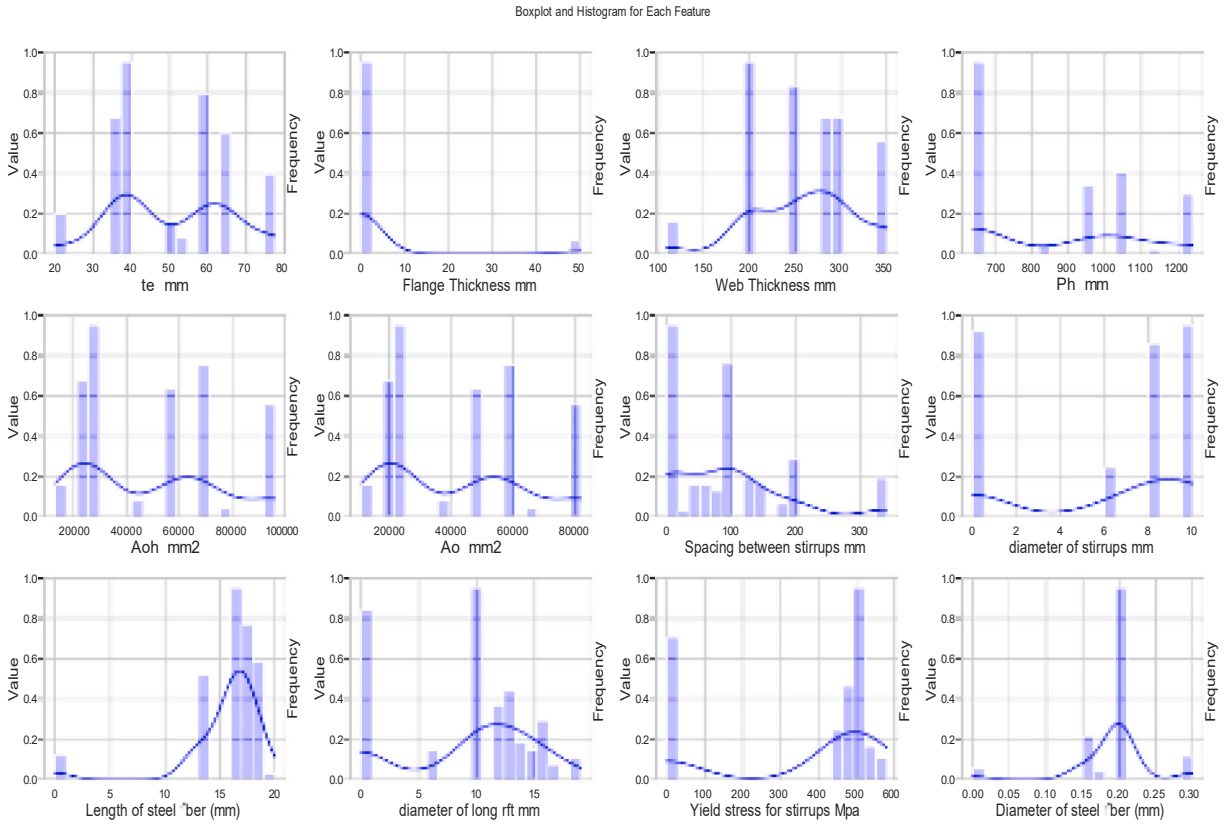

Fig. 1. Boxplots of some selected features.

2. Data Preprocessing
3. Model development (training)
4. Model performance evaluation (testing)

3.1. Data collection

The following subsection explains the dataset used in this study to predict the torsional behavior of UHPC with machine learning methods. These selected specimens and their features serve as the foundation for developing and evaluating prediction models. The dataset for this investigation consists of 113 UHPC beam specimens subjected to pure torsion. This dataset was obtained from the available research publications and experimental studies [21–31]. These specimens represent a wide variety of UHPC compositions, geometries, and reinforcement configurations, representing the practical variances found in real world constructions. Each specimen entry comprises 30 key parameters, encompassing:

- Geometric properties: Web width, web thickness, flange width, flange thickness, the perimeter of outermost stirrups (Ph), the area enclosed by outermost stirrups (Aoh), the area enclosed by shear flow (Ao), the effective thickness of the concrete section (te), spacing between stirrups, the diameter of stirrups.
- Reinforcement properties: Number of longitudinal reinforcement bars, diameter of longitudinal reinforcement bars, yield stress for stirrups, yield stress for longitudinal reinforcement, transverse steel ratio, longitudinal steel ratio.
- Material properties: Steel fiber volume, silica fume content, w/c ratio, quartz sand content, cement content, superplastizer content, curing time at natural temperature, curing time at 90°C, length of steel fiber, diameter of steel fiber, tensile strength of steel fiber.
- Mechanical properties: Cylindrical compressive strength, splitting tensile strength, modulus of elasticity.

3.2. Data preprocessing

This study analyzed data normality for each parameter by assessing skewness and kurtosis, which provide insight into the distribution's shape and symmetry. Given the dataset size (113 samples), verifying normality is essential. Skewness evaluates distribution asymmetry relative to the median [49], while kurtosis measures peakiness or flatness compared to a normal distribution [50].

Table 2
Features Importance.

Features	Importance
te mm	0.299272
Length of steel fiber (mm)	0.091892
Cracking Angle of twist rad/m	0.054947
Splitting tensile strength (MPa)	0.017637
Diameter of stirrups	0.016687
Web Width mm	0.014174
Aoh mm2	0.011665
Crack Angle of inclination	0.008741

Table 3
Optimal Parameters for Different Models.

Model	Optimal Parameter	Parameter Space	Value
GBR	Number of Models	[100,200,500]	500
	Maximum Depth	[3,5,6,10]	6
	Minimum Samples Split	[2,3,5]	3
	Learning Rate	[0.001, 0.005, 0.006]	0.006
	Loss Function	[Squared E, Absolut E]	squared error
LSTM	Epochs	[20,30,50]	30
	Batch Size	[50,70,100]	70
	Verbose	[0, 1, 2]	2
	Shuffle	[True, False]	False
RF	Number of Trees	[100,200,300]	100
	Maximum Depth	[None, 10, 20]	None
	Minimum Samples Split	[2,5,10]	2
	Minimum Samples Leaf	[1–3]	1

Equations for these calculations are provided.

$$Skewness = \gamma_1 \frac{E[(X-\mu)^3]}{\sigma^3} \tag{1}$$

$$Kurtosis = \gamma_2 \frac{E[(X-\mu)^4]}{\sigma^4} \tag{2}$$

Where: E denotes the expected value. X is the random variable. μ is the mean of the distribution. γ is the standard deviation of the distribution Fundamental to data verification is the identification and resolution of missing data. In this context, a mechanism termed the" missingness matrix" is employed. This matrix facilitates the systematic identification of missing values, enabling the implementation of appropriate strategies for their replacement or handling the outcome of this technique will be presented in the next section.

3.2.1. Features selection

The initial selection of 30 parameters as input variables for predicting torsional strength was determined through literature review and previous studies. To address the issue of high dimensionality, further analysis was conducted to refine the feature set. Exploratory data analysis was performed to examine the distribution of each feature, with histograms provided as a visual representation in Fig. 1.

A tree-based model utilizing the Random Forest algorithm was then used to quantify the importance of each feature in predicting torsional strength. The obtained importance scores were summarized in Table 2 and used as a basis for refining the feature set, aiming for an optimal balance between model complexity and prediction accuracy.

The results of the feature importance analysis have identified several key parameters that significantly impact the prediction of torsional strength in Ultra- High-Performance Concrete (UHPC) models. The most influential factor is the thickness of the concrete element (te, mm), followed by the length of steel fiber (mm) and the cracking angle of twist (rad/m). Additionally, the splitting

tensile strength (f't, MPa) and diameter of stirrups also play important roles in influencing torsional capacity. The web width (mm), area of the opening (Aoh, mm^2), and crack angle of inclination (degrees) contribute to a lesser extent. Including these parameters in our predictive models enhances their accuracy and aligns them with the underlying mechanics of UHPC. By considering these critical factors, we can improve the reliability and precision of torsional strength predictions for UHPC in practical applications.

3.3. Model validation

The validation of our model consists of three main parts. First, we split the dataset into a training set (70 % of the data) and a test set (30 % of the data). This split helps prevent overfitting by ensuring the model doesn't learn too much noise from the training data and

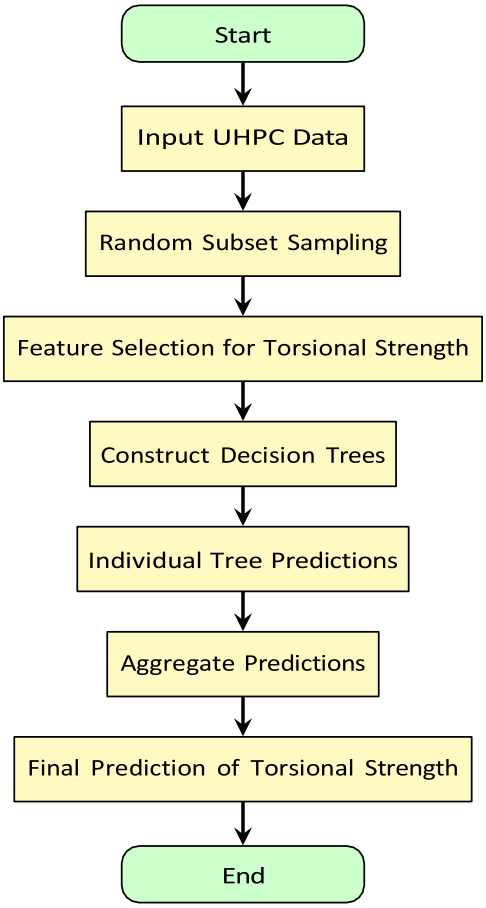

Fig. 2. Random Forest algorithm flowchart.

provides statistical validity for our evaluation metrics with a reliable test set size. Additionally, we used K-fold cross-validation with K= 3, which involves dividing the training data into three subsets and training the model three times, each time using a different subset for validation while training on the remaining data. The study optimized hyperparameters for the three chosen models to better capture complex patterns and effectively learn temporal dependencies. Validation data was employed to ensure generalization, with details of the hyperparameter tuning outlined in Table 3

3.3.1. Model training

In this study, a supervised machine learning approach was employed to estimate the torsional strength of Ultra-High-Performance Concrete (UHPC). Rigorous

data preparation was undertaken to ensure the dataset's suitability, with a 70 % training set used for model development and a 30 % testing set reserved to evaluate performance on unseen data. The algorithms selected—Gradient Boosting Machine (GBM), Long Short-Term Memory (LSTM), and Random Forest—were chosen based on an extensive literature review, which highlighted their superior predictive accuracy for similar applications. However, it should be noted that existing literature has not yet explored the prediction of torsional strength in UHPC, positioning this study as the first to apply these algorithms to this specific mechanical property. This novel approach not only fills a gap in the research but also advances the application of machine learning in UHPC performance prediction.

3.3.2. Random forest

Random forest is an ensemble learning method that builds on the principle of a decision tree. The training process consists of building up several decision trees, which in combination provide a result. Each tree is trained with features from a random part of the data selected, but the final prediction is done by aggregating the predictions of different trees [51]. The mathematical formula for regression is as follows:

$$Y_{RF}(X) = \frac{1}{n}\sum_{i=1}^{n} Y_i(x) \tag{3}$$

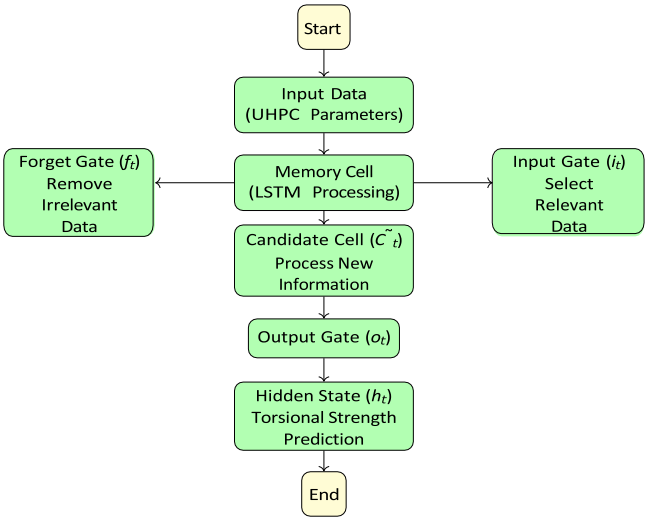

Fig. 3. LSTM Flowchart for Predicting Torsional Strength of UHPC.

Where $Y_i(X)$ is the prediction of the $(i)th$ decision tree for the input (X), and $Y_{RF}(X)$ is the aggregated prediction of the Random Forest. Fig. 2 provides a flowchart illustrating the framework of the Random Forest.

3.3.3. *Recurrent neural networks (LSTM)*

LSTM is a recurrent neural network (RNN) developed to handle sequential and time-series data. It is excellent at identifying long-term relationships and patterns within sequences. LSTMs employ memory cells and gates to selectively remember information, making them appropriate for tasks requiring temporal correlations [52]. The LSTM cell is made up of many gates and memory cells that control the flow of information. The LSTM equations for a single-time step are described below:

$$\begin{aligned} f_t &= \sigma(W_f \cdot [h_{t-1}, x_t] + b_f) \\ i_t &= \sigma(W_i \cdot [h_{t-1}, x_t] + b_i) \\ g_t &= tanh(W_g \cdot [h_{t-1}, x_t] + b_g) \\ c_t &= f_t \cdot c_{t-1} + i_t \cdot g_t \\ o_t &= \sigma(W_o \cdot [h_{t-1}, x_t] + b_o) \\ h_t &= o_t \cdot tanh(c_t) \end{aligned} \tag{4}$$

Where: σ represents the sigmoid activation function. W_f, W_i, W_g, and W_o are weight matrices associated with the forget gate, input gate, candidate cell state, and output gate, respectively. b_f, b_i, b_g, and b_o are bias vectors. The notation $[h_{t-1}, x_t]$ represents the concatenation of the previous hidden state h_{t-1} and the current input x_t. Fig. 3 illustrates the LSTM flowchart for predicting the torsional strength of UHPC.

3.3.4. *Gradient boosting regressor*

Gradient Boosting Regressor is a machine learning technique that sequentially creates an ensemble of weak learners [53], often decision trees. It seeks to remedy earlier model iterations' flaws by focusing on them in additional iterations. The final forecast is a weighted average of all individual model projections. Follows the mathematical formula for gradient boosting regressor:

$$F_m(x) = F_{m-1}(x) + v.h_m(x) \tag{5}$$

where: $F_m(x)$ is the output of the ensemble at iteration (m). $F_m - 1(x)$ is the output of the preceding iteration of the ensemble. μ is a positive constant representing the learning rate. $h_m(x)$ represents the prediction of the weak learner at iteration (m). Fig. 4 presents the Gradient Boosting flowchart for predicting the torsional strength of UHPC.

3.4. *Model performance evaluation*

Model performance was evaluated using the following metrics: Root Mean Square Error (RMSE), Mean Absolute Error (MAE), Coefficient of Determination (R^2), Mean Squared Error (MSE), and Mean Absolute Percentage Error (MAPE), as shown in Table 4. Each metric assesses different aspects of the model's accuracy.

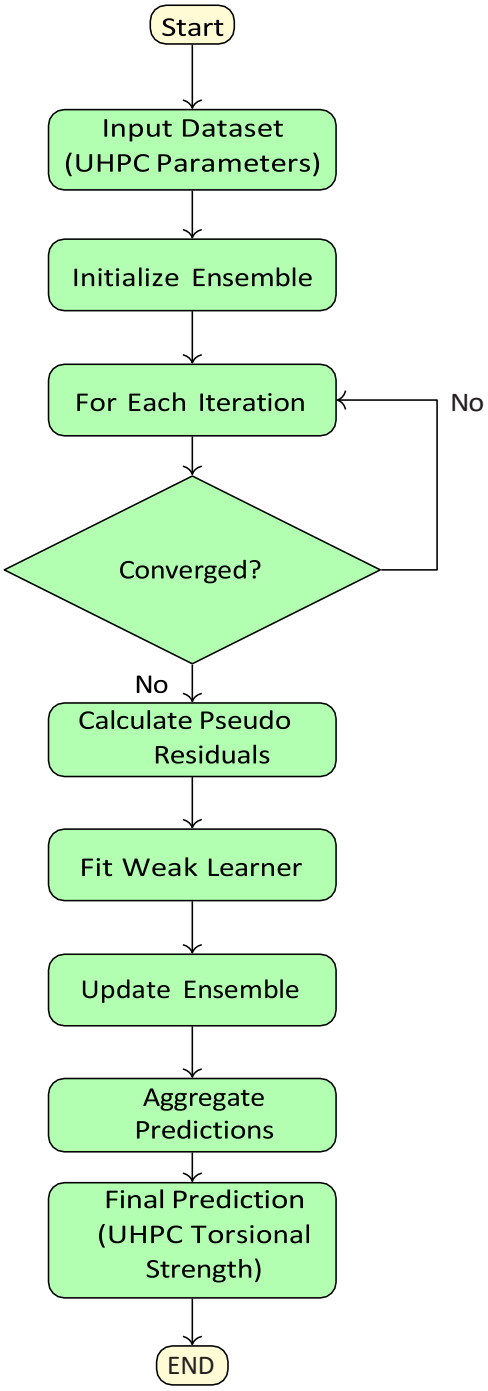

Fig. 4. Gradient Boosting Flowchart for Predicting Torsional Strength of UHPC.

4. Results

This section includes data preprocessing and model evaluation. Data preprocessing involves testing for normality and handling missing data. Model evaluation provides a comprehensive comparison of algorithm performance.

Table 4
Performance evaluation metrics.

Algorithms	Description
Coefficient of Determination [54]	In a regression model, it measures the fraction of the variation in the dependent variable that is explained by the independent variables. $R^2 = 1 - \frac{SS_{res}}{SS_{tot}}$ (6)
Mean Squared Error [55]	it computes the average squared difference between predicted and actual values. $MSE = \frac{1}{n}\sum_{i=1}^{n}(y_i - \hat{y}_i)^2$ (7)
Mean Absolute Percentage Error [56]	It's an indicator that calculates the average percentage difference between expected and actual values to assess the accuracy of a forecasting or prediction approach. $MAPE = \frac{1}{n}\sum_{i=1}^{n}\left\|\frac{y_i - \hat{y}_i}{y_i}\right\| \times 100$ (8)
Root Mean Square Error [55]	A statistic that quantifies the average size of deviations between expected and actual values. $RMSE = \sqrt{\frac{1}{n}\sum_{i=1}^{n}(y_i - \hat{y}_i)^2}$ (9)
Mean Absolute Error [55]	A metric that computes the average absolute differences between anticipated and actual values, providing a measure of prediction accuracy. $MAE = \frac{1}{n}\sum_{i=1}^{n}\|y_i - \hat{y}_i\|$ (10)

Table 5
Kurtosis and skewness values for all the parameters.

Parameters	Kurtosis	Skewness
Web Width mm	−1.15911	−0.168091
Flange Thickness mm	11.232601	3.637664
Ph mm	−1.419784	0.289039
Aoh mm2	−1.134505	0.419937
Ao mm2	−1.134505	0.419937
te mm	−0.940555	0.067881
Spacing between stirrups	1.166507	1.156103
diameter of stirrups mm	−1.390995	−0.606678
diameter of long rft mm	−0.889206	−0.590781
Yield stress for stirrups Mpa	−0.927346	−0.994694
Steel fiber volume Vf	−0.39963	1.141251
Silica fume, Sf	0.960048	0.835923
w/c ratio	0.752253	0.247622
Crack Angle of inclination	1.021599	−0.144728
Tcr	1.263301	1.38454
dCracking Angle of twist	32.608547	1.155299
Length of steel fiber	10.808148	0.6318531
Diameter of steel fiber	5.54256	5.666662
Tensile strength of steel fiber	15.74422	−3.972716
Tult	−0.173912	1.021456

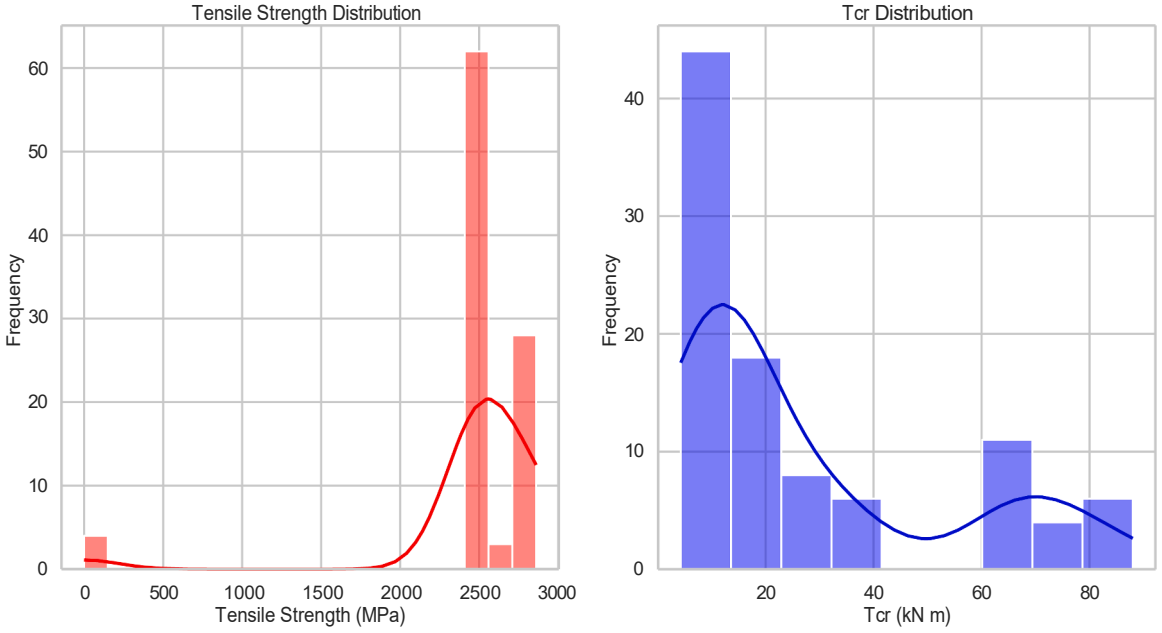

Fig. 5. Extraction of the distribution of some data parameters.

4.1. Data preprocessing

4.1.1. Normality test of the data

The major goal of this test was to determine whether the data had any impact on the effectiveness of developing the predictive model. Skewness and kurtosis metrics were used for this purpose. Following that, the gathered data for various statistical measures was synthesized and presented in a tabular as shown in Table 5.

Skewness and kurtosis were calculated to investigate the influence of data normality on the prediction model. These values, which are shown in Table 5, assess some parameters of data shape. Fig. 5 depicts a graphical review that provides insight into normalcy. During the analysis, all qualities were taken into account.

From the information presented in Table 5, it becomes evident that a wide range of skewness and kurtosis values exist. Focusing on skewness, it's important to note that negative values signify a left-skewed tail, whereas positive values indicate a right-skewed tail. For instance, attributes like web width, diameter of stirrups, and yield stress for stirrups exhibit negative skewness, indicating elongated left-side tails. On the other hand, parameters like flange thickness, diameter of steel fiber, and tensile strength of steel display positive

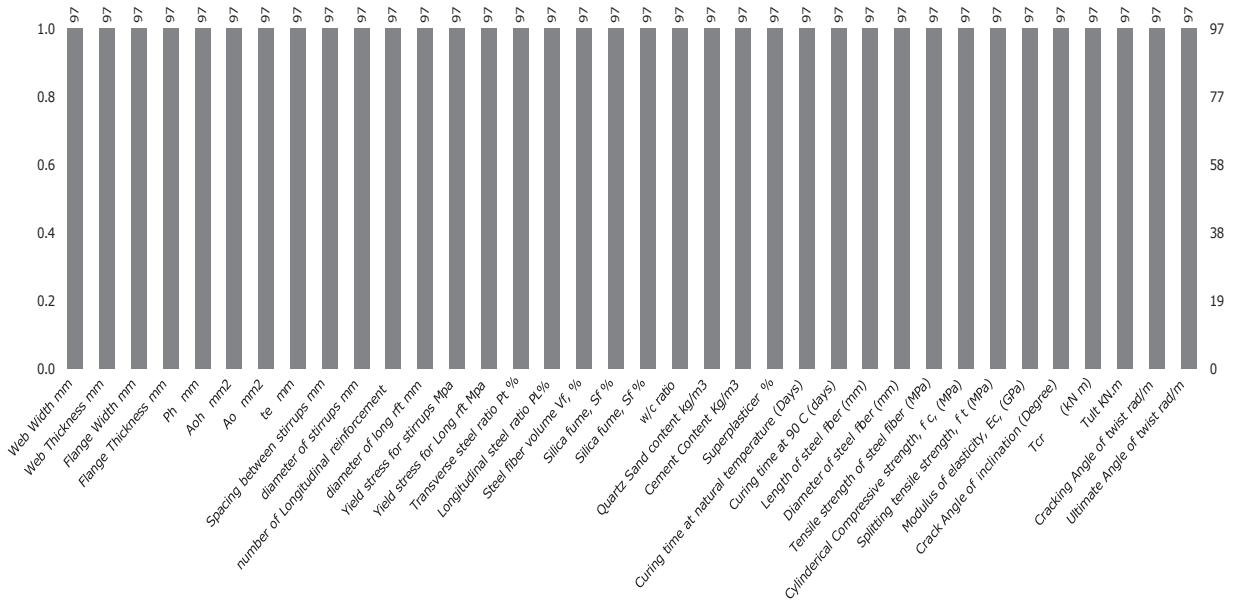

Fig. 6. matrix of missingness of the data.

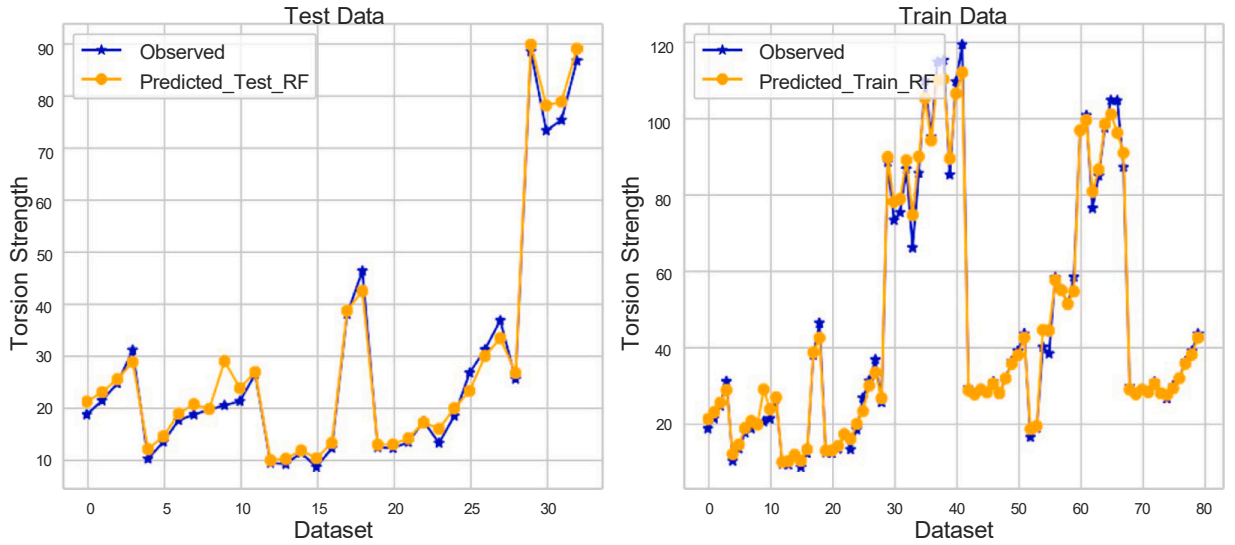

Fig. 7. Random Forest Predictions.

skewness, reflecting elongated right-side tails. Regarding kurtosis, a positive value signifies heavier tails compared to a normal distribution, indicating more extreme values and increased concentration around the mean. On the other hand, a negative value suggests lighter tails compared to a normal distribution, indicating fewer extreme values and less concentration around the mean. For instance, attributes

like flange thickness, cracking torque, and diameter of steel fiber exhibit positive kurtosis, pointing towards more extreme values and higher concentration around the mean. Conversely, attributes with negative kurtosis values, such as diameter of stirrups, crack angle of inclination, and tensile strength of steel fiber, imply fewer extreme values and lower concentration around the mean compared to a normal distribution. In a broad analysis guided by Table 4 and Fig. 5, it's apparent that the skewness values exhibit a bimodal density with a right-skewed orientation, indicating a normal asymmetry in the data. Concerning kurtosis, the distribution appears leptokurtic due to the majority of parameter values surpassing 0. This suggests increased variance in the data, leading to more pronounced peaks and heavier tails compared to a standard normal distribution.

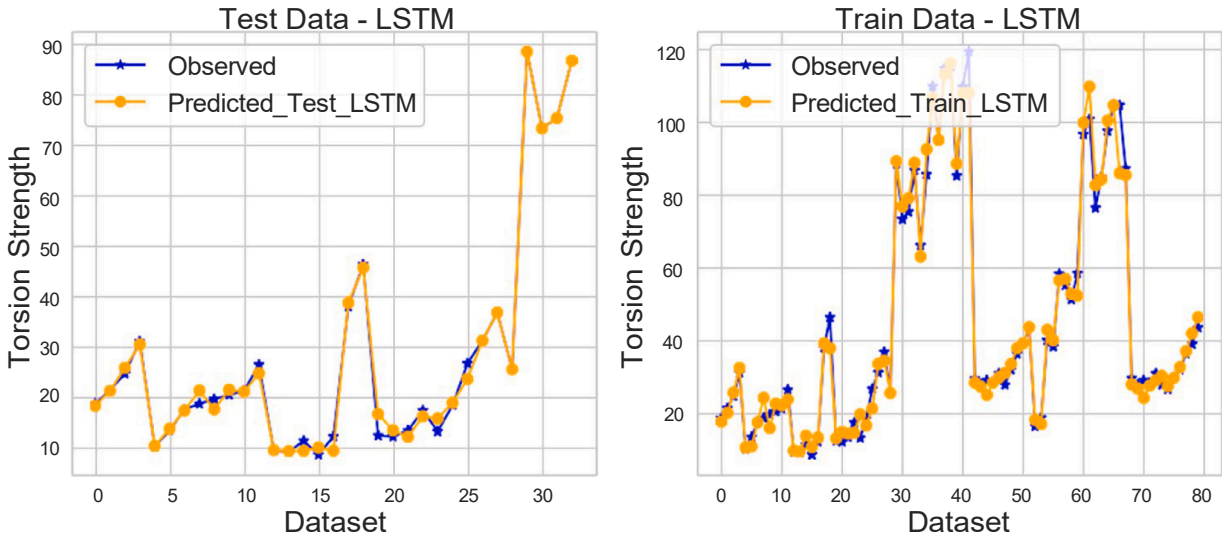

Fig. 8. LSTM Predictions.

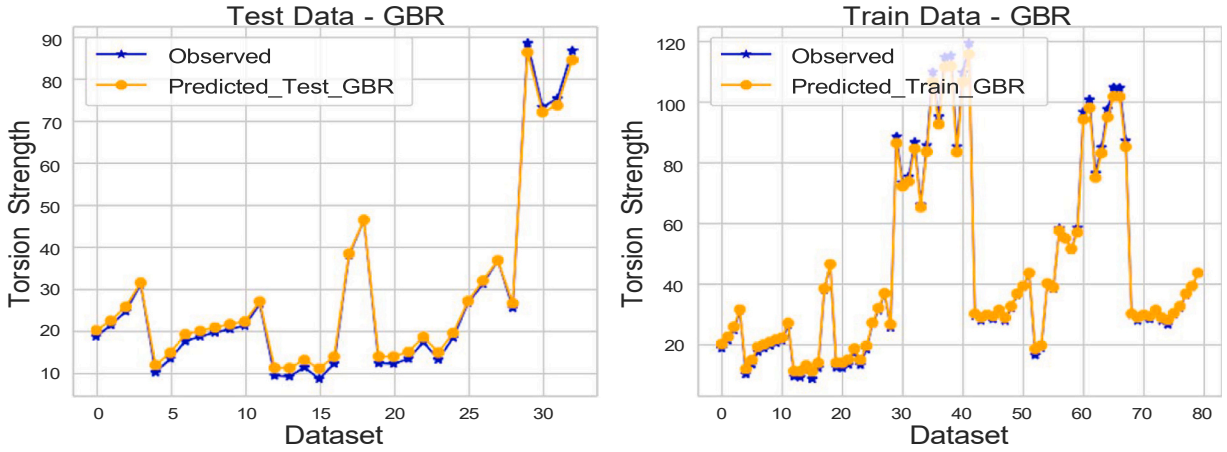

Fig. 9. GBR Predictions.

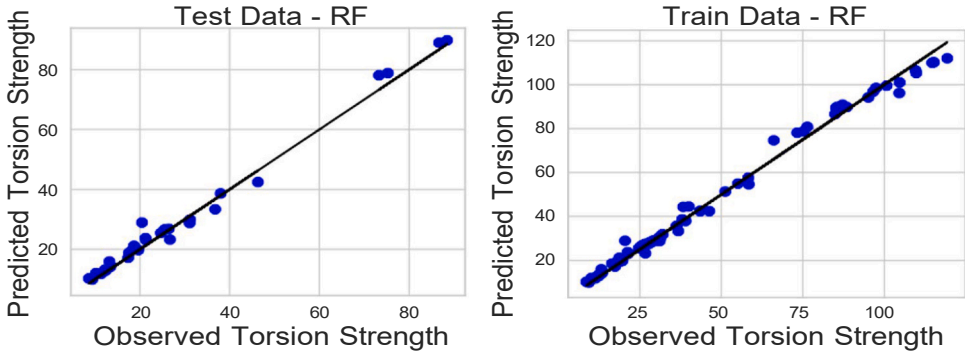

Fig. 10. Regression Line Between Actual and Predicted Values Using RF.

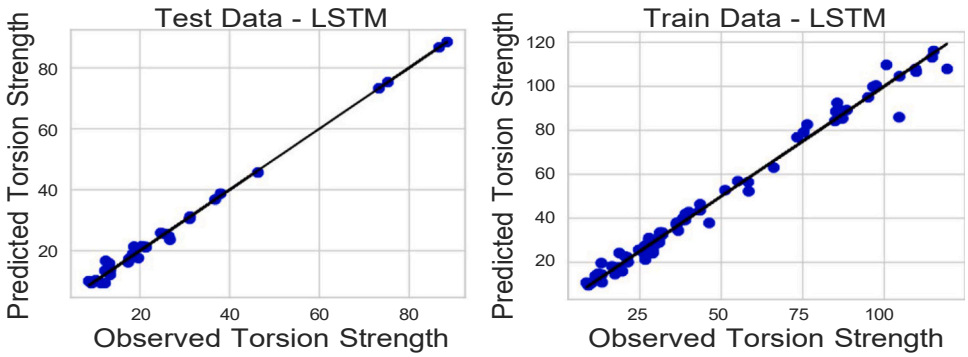

Fig. 11. Regression Line Between Actual and Predicted Values Using LSTM.

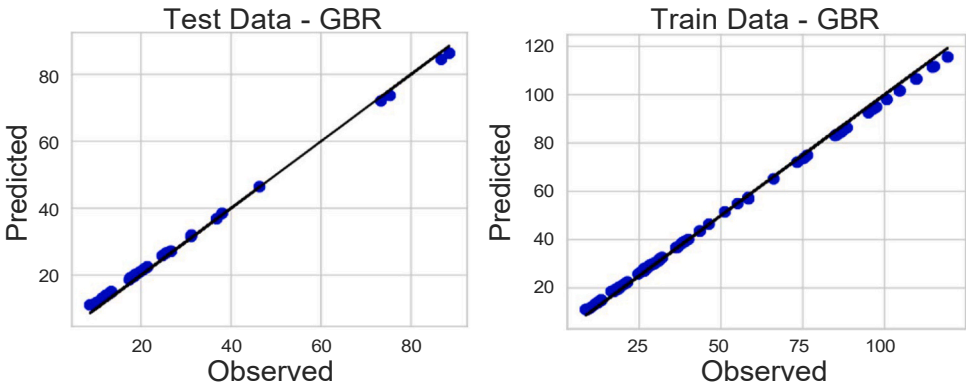

Fig. 12. Regression Line Between Actual and Predicted Values Using GBR.

Table 6
performance metrics for testing and training data.

	Random Forest	Long short-term memory	Gradient Boosting Regressor
R Squared Train	0.9341	0.976	0.973
RMSE Train	2.329	3.930	1.483
MAE Train	1.652	2.630	1.378
MAPE Train (%)	11.4	9.395	7.584
MSE Train	5.428	5.451	2.201
R Squared Test	0.958	0.967	0.987
RMSE Test	3.561	1.629	1.706
MAE Test	3.0501	1.210	1.466
MAPE Test (%)	10.2	8.743	8.200
MSE Test	9.303	2.654	2.912

4.1.2. Missingness of the data

As previously stated, the examination of data completeness aimed to assess the need for replacement in certain segments. As evident in Fig. 6, there is no missing data, with all values accounted for. To achieve this, a Python-based missingness matrix was employed for analysis.

4.2. Model evaluation

After applying the models (RF, LSTM, and GBR) and making predictions, we used performance metrics to compare predicted and actual values. For the Random Forest model, the correlation coefficient was 0.93, with an RMSE of 2.274, MAE of 1.646, MSE of 5.428, and MAPE of 11.4 %. The Long Short-Term Memory (LSTM) model improved on these metrics, achieving a correlation coefficient of 0.96, MAE of 1.213, RMSE of 1.621, MSE of 2.654, and MAPE of 9.395 %. The Gradient Boosting Regressor (GBR) demonstrated the highest accuracy,

with a 0.97 correlation coefficient, RMSE of 1.483, MAE of 1.378, MSE of 2.201, and MAPE of 7.584 %. Figs. 7–9 respectively

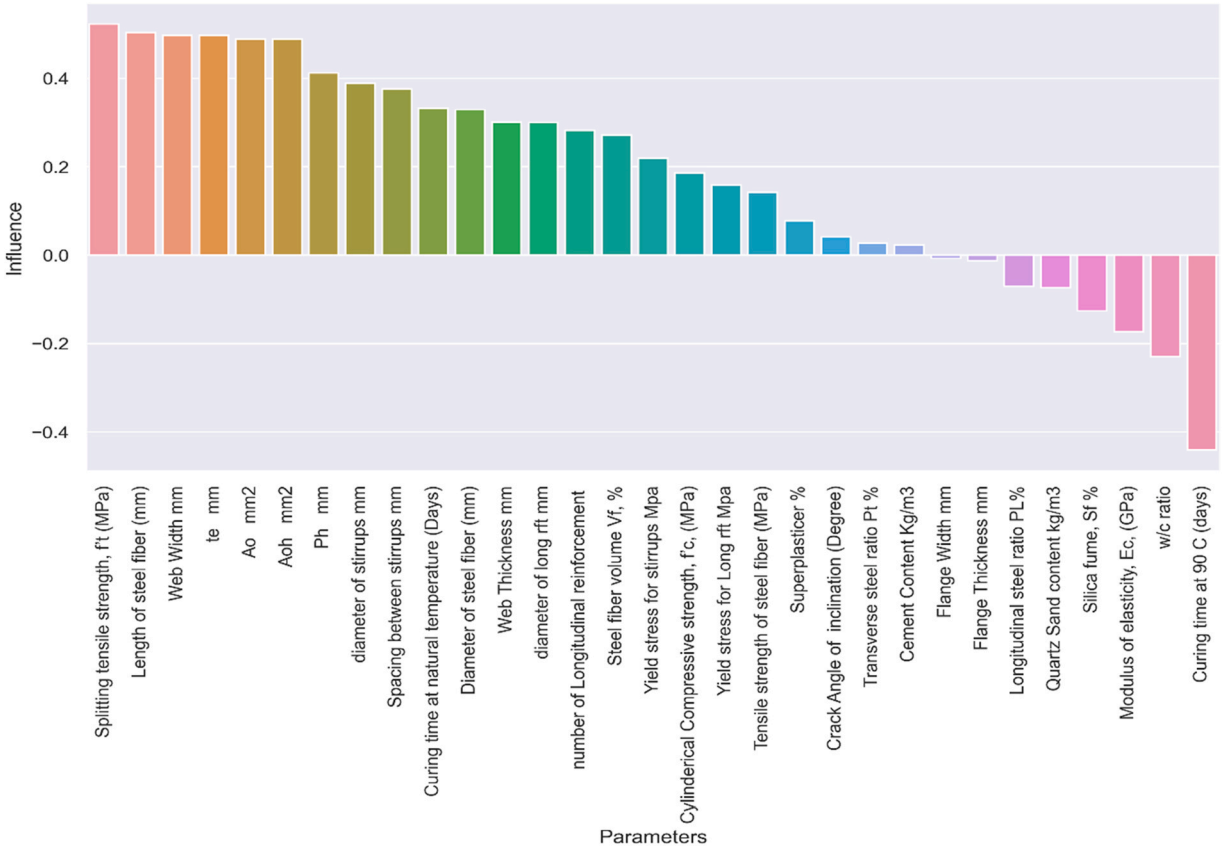

Fig. 13. Influence of each parameter.

Table 7
Summary of Correlation Methods and Equations.

Method	Description	Equation
Kendall Tau	Measure the correlation between two sets of ranked data, assessing the degree of agreement or discordance between ranks [66].	$\rho = 1 - \frac{C - D}{\frac{n(n-1)}{2}}$ (11)
Pearson correlation	Evaluates the linear relationship between two continuous variables X and Y by dividing their covariance by the product of their standard deviations [67].	$\rho = \frac{\sum (X_i - \widehat{X}).(\mathrm{Y_i} - \bar{\mathrm{Y}})}{\sqrt{\sum (X_i - \widehat{X})^2 . \sum (\mathrm{Y_i} - \bar{Y})^2}}$ (12)
Spearman rank correlation	Assesses the strength and direction of the relationship between two variables based on ranked data [68].	$\rho = 1 - \frac{6 - \sum d^2}{n(n^2 - 1)}$ (13)

provide combined comparisons of expected versus actual values, highlighting each model's predictive ability, while Figs. 10–12 illustrate their regression performances across training and testing phases. Together, these visuals analyze prediction accuracy and model effectiveness with real data.

Table 6 provides the evaluation metric values for both predicted and observed data for all three methods to give comprehensive information. This table provides a centralized reference for analyzing the performance of different algorithms based on multiple parameters, providing a complete overview of their prediction skills and alignment with actual data.

5. Discussion

The main objective of this study is to predict the effect of various parameters on the torsional strength of UHPC beams using three machine learning models: Gradient Boosting Regressor (GBR), Long Short-Term Memory (LSTM), and Random Forest (RF). While LSTM is a recurrent neural network, RF and GBR are ensemble methods. All three models outperformed benchmark results in the literature, with RF achieving an accuracy of 93 %, LSTM reaching 96 %, and GBR showing the highest accuracy at 97 %.

Among all identified parameters, the three algorithms highlighted splitting tensile strength, steel fiber length, web width, and stirrup diameter as the most influential factors affecting torsional strength. Fig. 13 visually ranks these parameters by their impact,

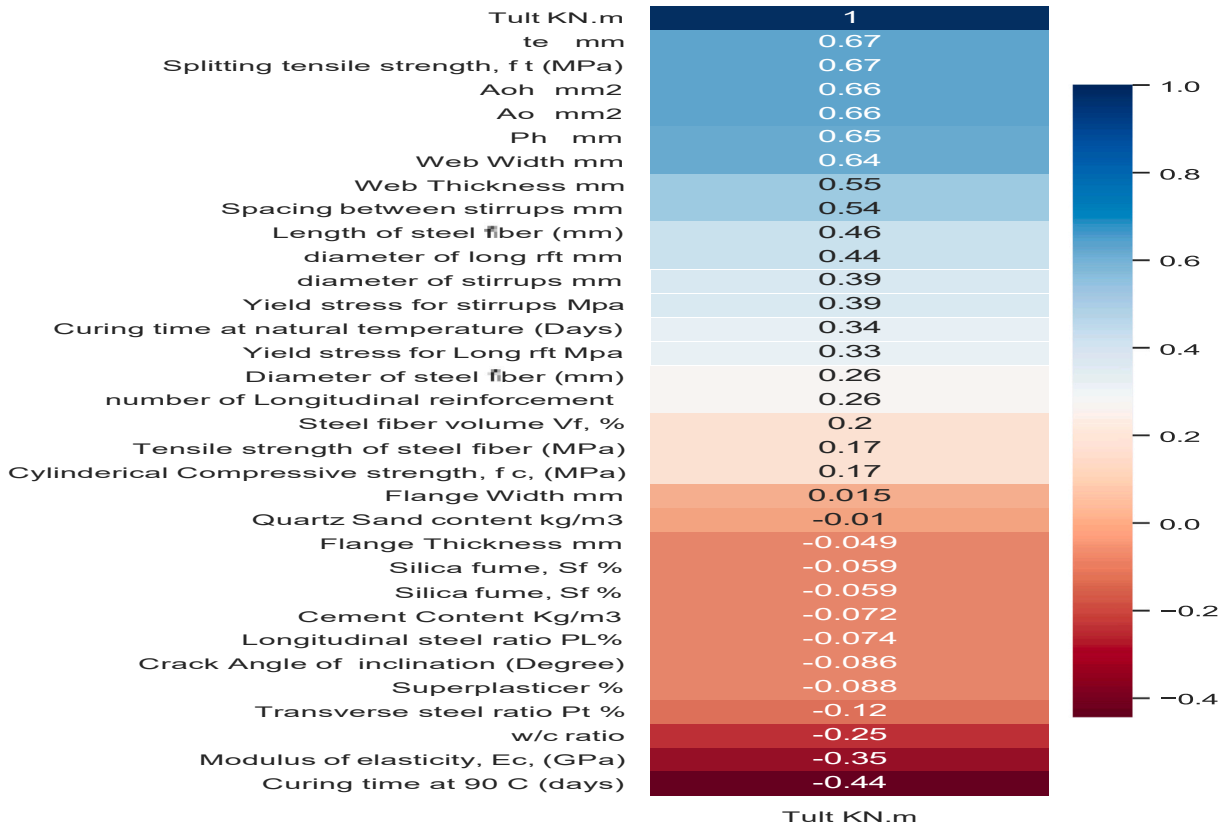

Fig. 14. Pearson correlation between torsion strength and UHPC parameters.

from most to least significant.

For clarity, a brief explanation of each commonly used performance measure of correlation, as listed in Table 7, is provided. These measures are further illustrated in Figs. 14–16.

Figs. 14,15,16 highlighted the key parameters that significantly influence the torsion strength, with splitting tensile strength, steel fiber length, web width, and stirrup diameter identified as the most impactful. According to correlation measures, splitting tensile strength ranks highest with an impact factor of 0.524, followed closely by steel fiber length at 0.50 and web width at 0.497. The other parameters that showed quite a considerable effect were the diameters of stirrups and steel fiber content, while flange thickness quartz sand content and silica fume are minor impact parameters. Interestingly, this result concerning respect to impact upon flange thickness and width seems conflicting with other studies [22,24,26] which show a significant improvement in ultimate torsional strength. Although the reasons for these might be in the early going of the current study—such as potentially a small sample size regarding flange variations—there remains a discrepancy here that warrants more investigation. Future research, considering a wider range of flange geometries, reinforcement configurations, and loading conditions, will be more capable of providing insight regarding the subtle effects flanges have on the torsional response of UHPC parameters and reconciling these conflicting viewpoints.

This section presents deeper insight on the five most influential parameters that have already been identified by elucidating their mechanisms in shaping the torsional behavior of UHPC. It also establishes a dialogue with previous research carried out by traditional methods.

- Splitting Tensile Strength: this is one of the very important parameters in resistance to cracking initiation and growth under torsional loads. The higher the tensile strength, the greater the material's capacity would be relative to the attainment of superior torsional performance by holding up to the development of torsion forces without cracks. Another positive influence there is due to steel fiber length, discussed below, such that longer fibers can act as an internal anchorage for more even distribution of stresses and increasing overall tensile strength. This agrees with the traditional experimental results where the tensile strength is a major factor that dictates the ultimate torsional capacity of UHPC [21,30].
- Steel Fiber Length: The longer the steel fibers, the better the internal reinforcement that would be realized by preventing crack propagation and enhancing load transfer within the matrix of UHPC. The increase in surface area of these fibers through length would mean better bonding with the matrix, which contributes towards torsional resistance. This further agrees with the theoretical models that longer fibers are quite effective in increasing crack resistance and general mechanical properties of UHPC [21–23].

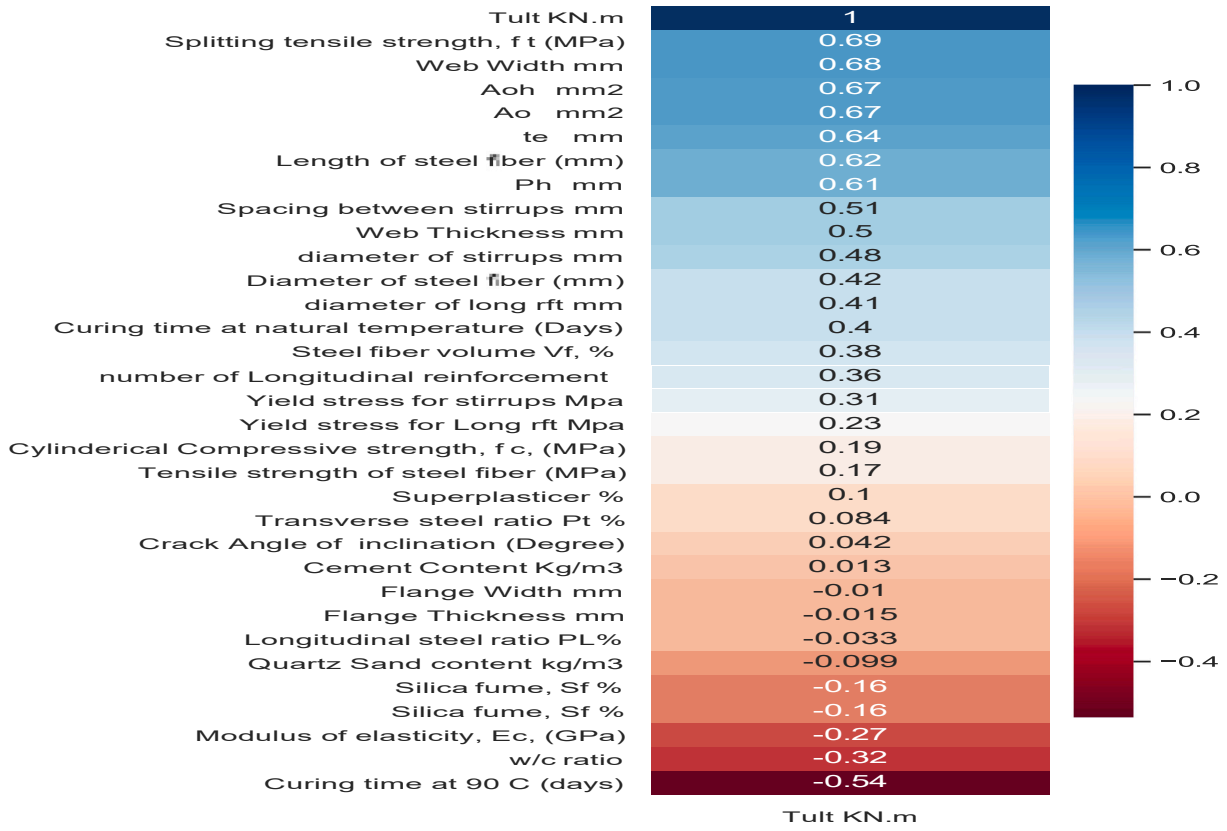

Fig. 15. spearman Rank correlation between torsion strength and UHPC parameters.

- Web Width: A wider web provides more surface area to resist torsional forces; otherwise, it gives a greater moment of inertia, and the UHPC has a better capacity not to yield when experiencing twisting deformations. This is consistent with previous works that accentuated that an increase in cross-sectional dimensions, containing web width, directly increases torsional capacity [22,24,25].
- Diameter of Stirrups: Stirrups control the transverse cracks by restraining the concrete under compression to avoid the cracks opening fully across the web. An increase in diameter increases the level of confinement, thus providing more resistance to major cracking and increasing the ultimate torsion strength. This further corroborates with past findings where the reinforced utilization of stirrups with steel fibers gives higher ultimate torsional strength and ductility for UHPC beams when compared to just leaning on steel fibers [23,27,28].
- Steel Fiber Volume High fiber volume brings about high density of internal reinforcement within the UHPC matrix. Inherently, this is translated to improved crack resistances, load-carrying capacities, and ultimately better torsional performance. The result is in line with the previous research findings that emphasize the positive impact of higher fiber volume on the mechanical properties of UHPC, including its torsional resistance.

The increasing agreement of results between the developed ML approach and conventional research methods, along with practical and theoretical models, is thereby beneficial for either method. This demonstrates how well the ML approach can capture and further predict the complex linkage concerning UHPC behavior. Classical methods are strongly supportive; they will give great insights apart from purely theoretical understanding, but ML powerfully supports data- driven analysis and optimization of UHPC design.

To validate the previously highlighted key parameters influencing torsional strength, the same algorithms were applied to a focused subset of the top 10 most impactful variables. This approach serves a dual purpose: verifying the effectiveness of the initial findings and gaining a deeper understanding of their relative importance. The ten chosen parameters, carefully selected for their significant influence, encompass a wide range of factors crucial to torsional behavior. The results of this implementation are shown in Table 8 and Figs. 17 and 18, which display the performance metrics and regression lines for both training and testing data across the three algorithms. These results closely match those in Table 6, demonstrating the model's robustness and consistency across different parameter sets .

Based on the results from Table 6 and Fig. 18, we remark that Gradient Boosting Regressor comes good with an R-squared of 99 %, which means it shows an excellent fit between the predictions by the model and the values. Besides that, there is an important decrease in other errors of metrics like RMSE, MAE, and MAPE. Long Short-Term Memory is the next best model in terms of accuracy, which got second place after the CNN, with a rate of precision at 98 %. The high value of R-squared is also well supported by other performance

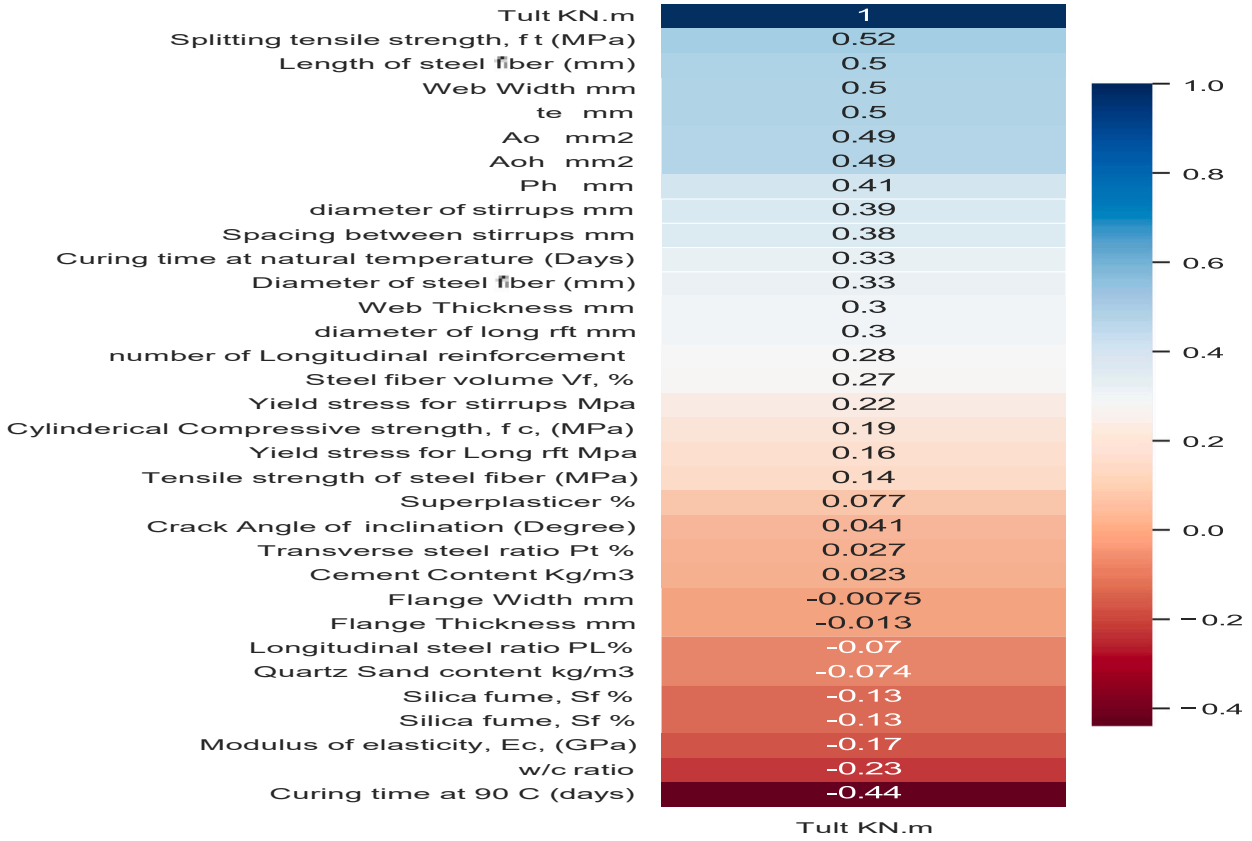

Fig. 16. Kendall Tau between torsion strength and UHPC parameters.

Table 8
performance metrics for testing and training data for the selected parameters.

	Random Forest	Long short-term memory	Gradient Boosting Regressor
R Squared Train	0.9641	0.980	0.988
RMSE Train	1.762	1.088	1.03
MAE Train	1.468	1.335	1.07
MAPE Train (%)	10.4	9.093	5.54
MSE Train	3.428	2.512	1.214
R Squared Test	0.959	0.973	0.990
RMSE Test	2.619	1.295	1.303
MAE Test	3.001	1.104	1.042
MAPE Test (%)	9.21	7.539	6.060
MSE Test	9.004	1.699	1.268

metrics with a clear decline, indicating improvement under predictive accuracy over and above the base dataset. In the case of the Random Forest, it is possible to ensure that it has a precision of 96 %, placing it in the third position, which shows how well it fits, even considering the complexity of the full dataset. Overall, such a review would be fundamental in selecting the best strategy for parameter influence prediction.

The reason we obtained these results is due to the strengths of the various models employed. The Gradient Boosting Regressor (GBR) is a highly accurate model attributed to its efficient loss function optimization and its ability to handle various data distributions, particularly since the data distribution was platykurtic. Furthermore, the selection of features through the three correlation metrics—Kendall tau, Pearson correlation, and Spearman rank correlation—had a significant impact on model training by accurately identifying the most influential parameters, thereby improving the overall predictive capability. In comparison, Long Short-Term Memory (LSTM) networks, which can learn temporal dependencies, excel in processing sequential and time-series data but have increased training complexity and require careful hyperparameter tuning. This may not always allow them to outperform tree-based models like GBR, especially when the relationships in the data lack strong temporal dynamics. Therefore, it's crucial to choose the appropriate model based on the underlying data characteristics and the specific problem being addressed.

Our Study, underscores the significant influence of an appropriately selected set of parameters on the ability to accurately predict

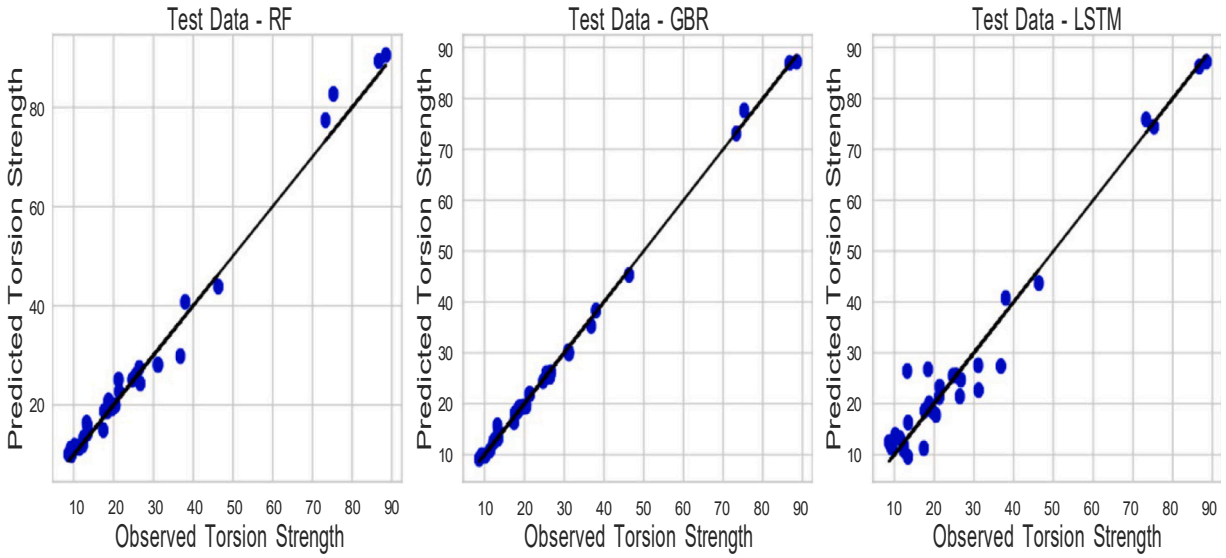

Fig. 17. Regression line of the three models.

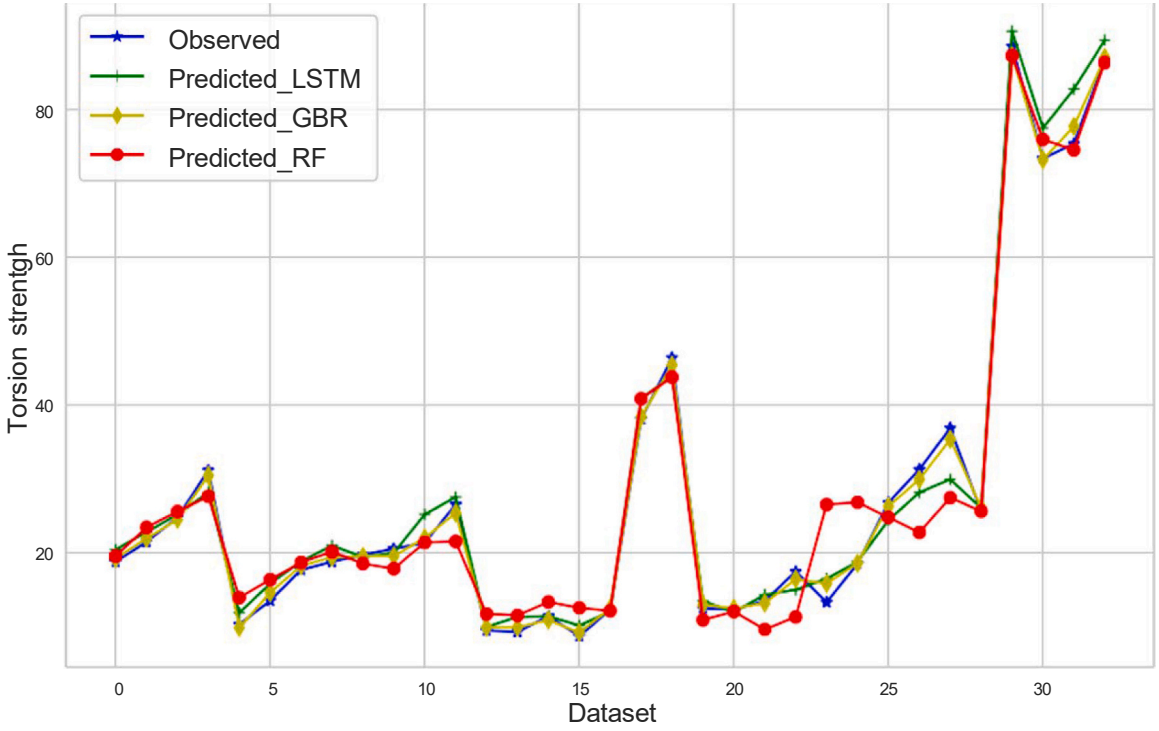

Fig. 18. Comparison between (RF, LSTM, GBR) in UHPC Torsion Strength.

the torsional strength of Ultra- High-Performance Concrete (UHPC), and the results of our study demonstrate a strong impact in this regard. This observation opens up promising avenues for optimizing the composition of UHPC. By strategically increasing the proportion of certain influential parameters—such as tensile strength, length of steel fiber,

and web width—it is possible to enhance the predictive accuracy and overall, performance of UHPC structures. Such advancements pave the way for a targeted approach to the design and optimization of UHPC, potentially leading to the development of stronger, more resilient, and more accurately predictable structures, thereby contributing to future improvements in construction and material science. In order to continue and develop our work, we will focus on several key areas to enhance the understanding and application of ultra-high-performance concrete (UHPC). Firstly, it is essential to apply and predict other structural behaviors of UHPC, such as shear

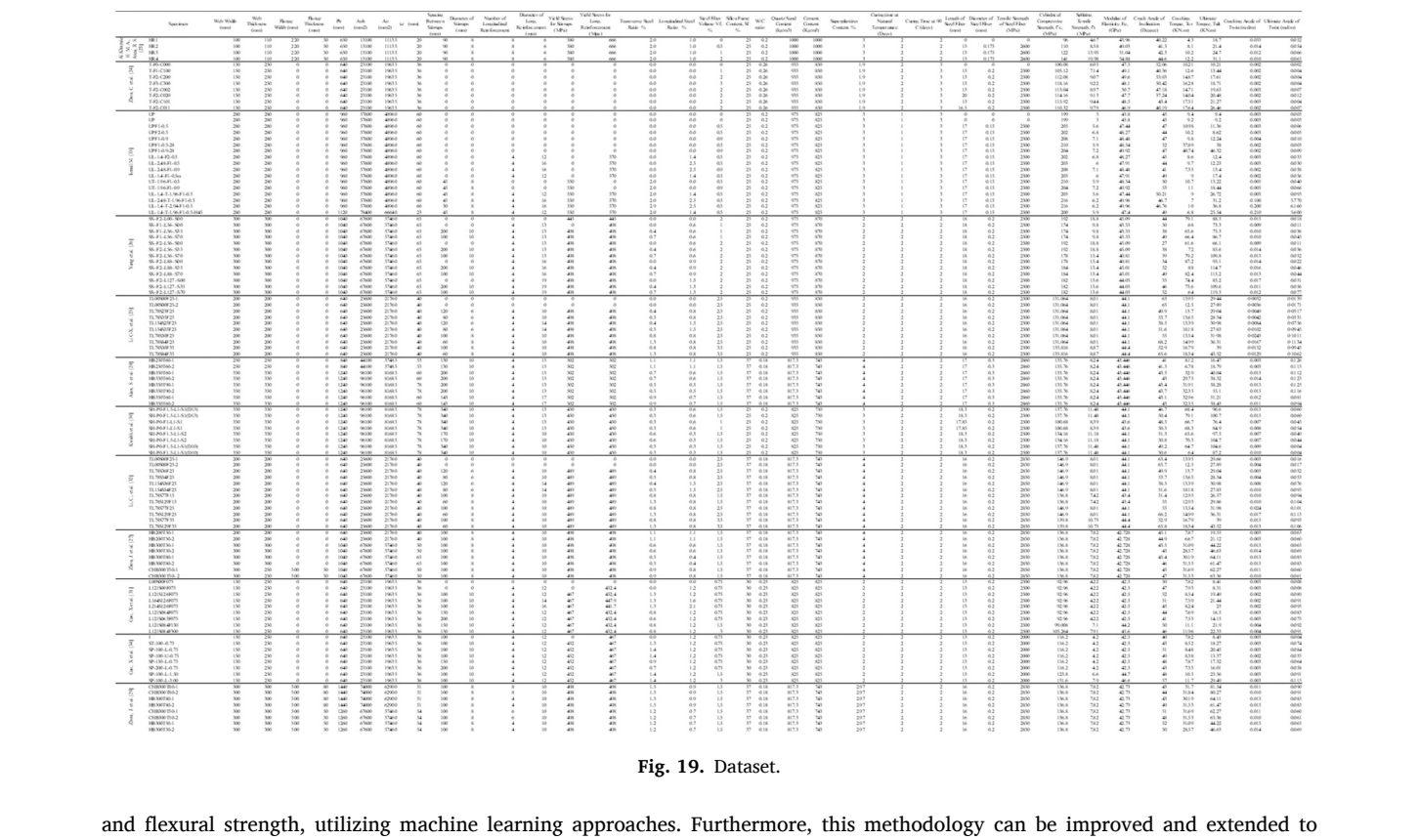

Fig. 19. Dataset.

and flexural strength, utilizing machine learning approaches. Furthermore, this methodology can be improved and extended to encompass other construction materials beyond UHPC. The development of ensemble models that integrate the capabilities of multiple algorithms could also enhance performance. Additionally, expanding the dataset to include a broader range of beam geometries, reinforcement details, and material types would contribute to more robust predictions. It is also important to investigate a wider variety of flange designs to better understand their subtle nuances in torsional behavior. Finally, incorporating data from various loading conditions, including combined loading situations, will provide a more comprehensive understanding of UHPC's performance under different scenarios.

6. Conclusion

The study reveals that parameter selection significantly impacts the prediction of the torsional strength of UHPC beams using machine learning algorithms. The results from three algorithms (Random Forest, LSTM, and Gradient Boosting Regressor) show that increasing fiber length and web width are the most significant factors influencing the torsional capacity of UHPC beams. Longer fibers distribute stresses more effectively and increase resistance to cracking, aligning with traditional research findings. A wider web also increases the moment of inertia, indicating the beam's resistance to bending and more space for the shear flow zone. Stirrup diameter plays a crucial role in the torsional behavior of UHPC beams, enhancing confinement and mitigating crack propagation.

The study also found that the presence of flanges does not significantly influence the torsional strength of UHPC beams, possibly due to the limited range of flange geometries used. Exploring diverse flange designs could reveal a more nuanced relationship with torsional behavior.

The Gradient Boosting Regressor algorithm was the top performer, with an R-squared value of 99.9 %, demonstrating its ability to align predictions of torsional behavior with actual values accurately. LSTM and Random Forest algorithms while occupying second and third positions, still deliver impressive precision rates of 98.5 % and 96.0 %, highlighting the approach's robustness across diverse algorithms.

CRediT authorship contribution statement

Khaoula Elhabyb: Writing – original draft, Visualization, Software, Project administration, Methodology. **Ahmad Awad:** Writing – original draft, Validation, Resources, Data curation, Conceptualization. **Mohammad Salama:** Writing – review & editing, Supervision, Project administration, Data curation. **Mostafa Bellafkih:** Validation, Project administration, Conceptualization. **Baina Amine:** Software, Project administration. **Amr El-Said:** Supervision, Funding acquisition. **Ahmad Farouk Deifalla:** Investigation, Funding acquisition, Formal analysis.

Declaration of Competing Interest

The authors declare that they have no known competing financial interests or personal relationships that could have appeared to influence the work reported in this paper.

Data availability

Data will be made available on request.

References

[1] M. Zhou, W. Lu, J. Song, G.C. Lee, Application of ultra-high performance concrete in bridge engineering, Constr. Build. Mater. 186 (2018) 1256–1267.
[2] S.H. Park, D.J. Kim, G.S. Ryu, K.T. Koh, Tensile behavior of ultra high performance hybrid fiber reinforced concrete, Cem. Concr. Compos. 34 (2012) 172–184, https://doi.org/10.1016/j.cemconcomp.2011.09.009.
[3] B. Graybeal, J. Tanesi, Durability of an ultrahigh-performance concrete, J. Mater. Civ. Eng. 19 (2007) 848–854.
[4] I.-H. Yang, C. Joh, B.-S. Kim, Flexural response predictions for ultra-high-performance fibre-reinforced concrete beams, Mag. Concr. Res 64 (2011) 113–127.
[5] R. Solhmirzaei, V. Kodur, Modeling the response of ultra high performance fiber reinforced concrete beams, Procedia Eng. 210 (2017) 211–219.
[6] C.-H. Jeng, S.-F. Peng, H.-J. Chiu, C.-K. Hsiao, New torsion experiment on large sized hollow reinforced concrete beams, Acids Struct. J. 111 (6) (2014) 1469–1480, https://doi.org/10.14359/51687166.
[7] T. Sathish, V. Mohanavel, Preparation and testing of fibre reinforced Zea mays and Calotropis gigantea concrete material under various testing conditions, Int. J. Rapid Manuf. 8 (1–2) (2019) 34–51.
[8] M. Schmidt, E. Fehling, Ultra-high-performance concrete: research, development and application in europe, Acids Spec. Publ. 228 (2005) 51–78.
[9] D. Wang, C. Shi, Z. Wu, J. Xiao, Z. Huang, Z. Fang, A review on ultra high performance concrete: Part II. Hydration, microstructure and properties, Constr. Build. Mater. 96 (2015) 368–377, https://doi.org/10.1016/j.conbuildmat.2015.08.095.
[10] L. Qing, K. Yu, R. Mu, J.P. Forth, Uniaxial tensile behavior of aligned steel fibre reinforced cementitious composites, Mater. Struct. 52 (4) (2019) 70, https://doi.org/10.1617/s11527-019-1374-5.
[11] D.-Y. Yoo, N. Banthia, Y.-S. Yoon, Predicting the flexural behavior of ultra- highperformance fiber-reinforced concrete, Cem. Concr. Compos 74 (2016) 71–87, https://doi.org/10.1016/j.cemconcomp.2016.09.005.
[12] L. Qing, Y. Li, X. Wang, K. Yu, R. Mu, Investigation of mixed-mode fracture of aligned steel fibre reinforced cementitious composites, Int J. Fract. 228 (2) (2021) 159–178, https://doi.org/10.1007/s10704-021-00527-w.
[13] L. Qing, Y. Cheng, R. Mu, Toughness enhancement and equivalent initial fracture toughness of cementitious composite reinforced with aligned steel fibres. Fatigue Fract. Eng. Mater. Struct. 42 (11) (2019) 2533–2543, https://doi.org/10.1111/ffe.13102.
[14] D.-Y. Yoo, S.-T. Kang, Y.-S. Yoon, Enhancing the flexural performance of ultra- high performance concrete using long steel fibers. Compos Struct. 147 (2016) 220–230, https://doi.org/10.1016/j.compstruct.2016.03.032.
[15] Z. Wu, K.H. Khayat, C. Shi, How do fiber shape and matrix composition af- fect fiber pullout behavior and flexural properties of UHPC? Cem. Concr. Compos 90 (2018) 193–201, https://doi.org/10.1016/j.cemconcomp.2018.03.021.
[16] L. Jin, R. Zhang, Y. Tian, G. Dou, X. Du, Experimental investigation on static and dynamic mechanical properties of steel fiber reinforced ultra-high-strength concretes, Constr. Build. Mater. 178 (2018) 102–111, https://doi.org/10.1016/j.conbuild- mat.2018.05.152.
[17] L. Qing, G. Cao, J. Guan, S. Li, Experimental method for determining the frac- ture toughness of concrete based on the modified two-parameter model and DIC technique. Fatigue Fract. Eng. Mater. Struct. 45 (2) (2022) 400–410, https://doi.org/10.1111/ffe.13602.
[18] X. Cao, Y.C. Ren, L. Zhang, et al., Flexural behavior of ultra-high performance concrete beams with various types of rebar, Compos. Struct. 292 (2022) 115674.
[19] K. Turker, I.B. Torun, Flexural performance of highly reinforced composite beams with ultra-high- performance fiber reinforced concrete layer, Eng. Struct. 219 (2020) 110722.
[20] Q. Wang, H.L. Song, C.L. Lu, et al., Shear performance of reinforced ultra-high performance concrete rectangular section beams, Structures 27 (8) (2020) 1184–1194.
[21] X. Cao, Y.C. Ren, K. Qian, et al., Size effect on flexural behavior of ultra-high per- formance concrete beams with different reinforcement, Structures 41 (2022) 969–981.
[22] Y. Zhu, Y. Zhang, H.H. Hussein, G. Chen, Flexural strengthening of reinforced concrete beams or slabs using ultra-high performance concrete(UHPC): a state of the art review, Eng. Struct. 205 (2020) 110035, https://doi.org/10.1016/j.en-gstruct.2019.110035.
[23] C.-X. Li, Z. Feng, L. Ke, et al., Experimental study on shear performance of cast-in-place ultra-high performance concrete structures, Mater 12 (19) (2019) 3254, https://doi.org/10.3390/ma12193254.
[24] C. Zhou, J. Wang, W. Jia, Z. Fang, Torsional behavior of ultra-high performance concrete (UHPC) rectangular beams without steel reinforcement: ex- perimental investigation and theoretical analysis, Compos. Struct. 299 (2022) 116022, https://doi.org/10.1016/j.compstruct.2022.116022.
[25] H.M.A. Al.Khuzaie, R.S. Atea, Investigation of torsional behavior and capacity of reactive powder concrete (RPC) of hollow T-beam, J. Mater. Res. Technol. 8 (1) (2019) 199–207, https://doi.org/10.1016/j.jmrt.2017.10.008.
[26] I.H. Yang, C. Joh, J.W. Lee, et al., Torsional behavior of ultra-high performance concrete squared beams, Eng. Struct. 56 (2013) 372–383.
[27] J. Zhou, C. Li, Z. Feng, D.-Y. Yoo, Experimental in- vestigation on torsional behaviors of ultra-high-performance fiber-reinforced concrete hollow beams, Cem. Concr. Compos. 129 (2022) 104504, https://doi.org/10.1016/j.cemconcomp.2022.104504.
[28] S. Alan, M.A. Kumar, T.S.R. Babu, P. Madhan, R. Venkatra- man, R. SrinivasPrabhu, Investigation of torsional effect of UH- PFR concrete hollow beams, Mater. Today. Proc. 69 (2022) 1110–1117, https://doi.org/10.1016/j.matpr.2022.08.175.
[29] J. Zhou, P. Yu, D.-Y. Yoo, L. Yu, L. Ke, Effectiveness of flange plates on torsional behaviors of ultra-high-performance fiber-reinforced concrete hollow beams, Dev. Built Environ. 16 (2023) 100227, https://doi.org/10.1016/j.dibe.2023.100227.
[30] I. Kwahk, C. Joh, J.W. Lee, Torsional behavior design of UHPC box beams based on thin-walled tube theory, Engineering 7 (3) (2015) 101–114.
[31] X. Cao, W.-J. Zhang, Y.-C. Ren, F. Fu, Y.-H. Li, D.-B. He, Y. Zheng, Torsional capacity of ultra-high-performance concrete beams using rectangle stirrup, J. Build. Eng. 69 (2023) 106231, https://doi.org/10.1016/j.jobe.2023.106231.
[32] C. Li, J. Zhou, L. Ke, S. Yu, H. Li, Failure mechanisms and loading capacity prediction for rectangular UHPC beams under pure torsion. Eng. Struct. 264 (2022) 114426 https://doi.org/10.1016/j.engstruct.2022.114426.
[33] J.G. Mitobaba, X. Wu, B. Chen, J. Su, Z. Dong, A modified space truss analogy model for ultimate torsional capacity of ultra-high-performance con- crete solid and box beams, Adv. Struct. Eng. 25 (12) (2022) 2427–2443, https://doi.org/10.1177/13694332221099405.
[34] X. Cao, Y.-P. Quan, Y.-C. Ren, F. Fu, Q.-Z. Jin, D.-B. He, Y. Zheng, Experiment study on reactive powder concrete beams using spirals reinforcement under torsion, Eng. Struct. 290 (2023) 116361, https://doi.org/10.1016/j.engstruct.2023.116361.
[35] S. a R. Shah, M. Azab, H.M. Seif Eldin, O. Barakat, M.K. Anwar, Y. Bashir, Predicting compressive strength of blast furnace slag and fly ash based sustainable concrete using machine learning techniques: an application of advanced decision-making approaches, Buildings 12 (2022) 914, https://doi.org/10.3390/buildings12070914.
[36] Y. Qian, M. Sufian, A. Hakamy, A. Farouk Deifalla, A. El-said, Application of machine learning algorithms to evaluate the influence of various parameters on the flexural strength of ultra-high-performance concrete, Front. Mater. 9 (2023) 1114510, https://doi.org/10.3389/fmats.2022.1114510.

[37] Q. Wang, A. Hussain, M.U. Farooqi, A.F. Deifalla, Artificial intelligence-based estimation of ultra-high-strength concrete's flexural property, Case Stud. Constr. Mater. 17 (2022) e01243, https://doi.org/10.1016/j.cscm.2022.e01243.
[38] Yunfeng Qian, Sufian Muhammad, Hakamy Ahmad, Deifalla Ahmed Farouk, Amr El-Said, Application of machine learning algorithms to evaluate the influence of various parameters on the flexural strength of ultra-high-performance concrete, Front. Mater. 9 (2023) 1114510.
[39] Ayaz Ahmad, Ahmad Waqas, Aslam Fahid, Joyklad Panuwat, Compres- sive strength prediction of fly ash-based geopolymer concrete via advanced machine learning techniques. Case Stud. Constr. Mater. 16 (2022) e00840.
[40] Guorui Sun, Du Maohua, Shan Baohua, Shi Jun, Qu Yiwen, Ultra-high performance concrete design method based on machine learning model and steel slag powder, Case Stud. Constr. Mater. 17 (2022) e01682.
[41] Jesus de-Prado-Gil, Palencia Covadonga, Silva-Monteiro Neemias, Martínez-García Rebeca, To predict the compressive strength of self-compacting concrete with recycled aggregates utilizing ensemble machine learning models, Case Stud. Constr. Mater. 16 (2022) e01046.
[42] Ning Zhang, Shen Shui-Long, Zhou Annan, Jin Yin-Fu, Application of LSTM approach for modelling stress–strain behaviour of soil. Appl. Soft Comput. 100 (2021) 106959.
[43] A. Tanhadoust, T.Y. Yang, Farshad Dabbaghi, Hwa Kian Chai, M. Mohseni, S.B. Emadi, S. Nasrollahpour, Predicting stress-strain behavior of normal weight and lightweight aggregate concrete exposed to high temperature using LSTM recurrent neural network, Constr. Build. Mater. 362 (2023) 129703.
[44] Qichen Wang, Hussain Abasal, Usman Farooqi Muhammad, Farouk Deifalla Ahmed, Artificial intelligence-based estimation of ultra-high-strength concrete's flexural property, Case Stud. Constr. Mater. 17 (2022) e01243.
[45] Paul O. Awoyera, S.Kirgiz Mehmet, A. Viloria, D. Ovallos-Gazabon, Es- timating strength properties of geopolymer self-compacting concrete using machine learning techniques, J. Mater. Res. Technol. 9 (4) (2020) 9016–9028.
[46] Mohammad Hematibahar, Kharun Makhmud, N.Beskopylny Alexey, A.Stel'makh Sergey, M.Shcherban' Evgenii, Razveeva Irina, Analysis of models to pre- dict mechanical properties of high-performance and ultra-high-performance con- crete using machine learning, J. Compos. Sci. 8 (8) (2024) 287.
[47] Chen, Shenggang, Congcong Chen, Shengyuan Li, Junying Guo, Quanquan Guo, and Chaolai Li. Predicting torsional capacity of reinforced concrete members by data-driven machine learning models. Frontiers of Structural and Civil Engineering (2024): 1-17.
[48] Shenggang Chen, Quanquan Guo, Yingying Zhang, Hexiang Hu, Bei Shen, Machine learning models for cracking torque and pre-cracking stiffness of RC beams, Arch. Civ. Mech. Eng. 23 1 (2022) 6.
[49] David P. Doane, E.Seward Lori, Measuring skewness: a forgotten statistic? J. Stat. Educ. 19 (2) (2011).
[50] Balanda, P. Kevin, H.L. MacGillivray, Kurtosis: a critical review, Am. Stat. 42 (2) (1988) 111–119.
[51] Liu, Yanli, Yourong Wang, and Jian Zhang. New machine learning algorithm: Random forest. In Information Computing and Applications: Third International Conference, ICICA 2012, Chengde, China, September 14-16, 2012. Proceedings 3, pp. 246-252. Springer Berlin Heidelberg, 2012.
[52] Staudemeyer, Ralf C., and Eric Rothstein Morris. Understanding LSTM–a tu- torial into long short-term memory recurrent neural networks. arXiv preprint arXiv: 1909.09586 (2019).
[53] Alexey Natekin, Alois Knoll, Gradient boosting machines, a tutorial. Front, Neurorobot. 7 (2013) 21.
[54] Gireen Naidu, Zuva Tranos, Mmbongeni Sibanda Elias, A review of evalua- tion metrics in machine learning algorithms. Computer Science On-line Confer- ence, Springer International Publishing, Cham, 2023, pp. 15–25.
[55] Tianfeng Chai, R.Draxler Roland, Root mean square error (RMSE) or mean absolute error (MAE)?–Arguments against avoiding RMSE in the literature, Geosci. Model Dev. 7 (3) (2014) 1247–1250.
[56] De. Myttenaere Arnaud, Boris Golden, B.énédicte Le Grand, Fabrice Rossi, Mean absolute percentage error for regression models. Neurocomputing 192 (2016) 38–48.